

# INVESTIGATION OF READOUT METHODS FOR ELECTRO-OPTICAL BEAM POSITION MONITOR PICKUPS

D. M. Harryman<sup>\*,1</sup>, M. Z. C. Bosman<sup>1</sup>, S. M. Gibson<sup>1</sup>

T. Lefèvre<sup>2</sup>, T. E. Levens<sup>2</sup>, A. Schlögelhofer<sup>2</sup>, G. Tangari<sup>2,3</sup>

<sup>1</sup>John Adams Institute, Royal Holloway, University of London, Egham, UK

<sup>2</sup>CERN, Geneva, Switzerland

<sup>3</sup>Sapienza University of Rome, Rome, Italy

## Abstract

Electro-optical pickups are being explored at CERN for the development of a high-bandwidth ( $\geq 5$  GHz) beam position monitor capable of measuring intra-bunch beam position. To support this effort, a prototype electro-optical beam position monitor has been installed in the Super Proton Synchrotron. The installation utilises a fibre-coupled laser directed into lithium niobate crystals. As the beam passes a crystal, its electromagnetic field induces a proportional phase shift in the laser light by altering the refractive index of the crystal. Signal readout is typically performed using multiple Mach-Zehnder interferometers, with crystals placed on either side of the beam. This configuration currently faces challenges, including baseline instability and limited dynamic range. This paper examines and evaluates methods and techniques for reading out the beam position from the phase-shifted laser to mitigate these limitations.

## INTRODUCTION

An Electro-Optical Beam Position Monitor (EO-BPM) system has been installed in the Super Proton Synchrotron (SPS) accelerator since 2024 [1]. This Beam Position Monitor (BPM) uses two fibre-coupled Lithium Niobate (LNB) crystals integrated into button pickup assemblies where a 780 nm Continuous Wave (CW) laser is injected into the crystals. As the particle beam passes by, its electric field modulates the phase of the laser light by changing the refractive index of each crystal proportionally. A signal of varying optical amplitude is produced and measured from these phase shifts by placing the LNB crystals into a Mach-Zehnder (MZ) interferometer configuration. Detailed descriptions of pickup development and EO-BPM operating principles appear in [1–5].

The SPS system employs three MZ interferometers, shown in Fig. 1, to generate signals for the difference channel ( $\Delta$ ), the left side-mode ( $L$ ), and the right side-mode ( $R$ ). Optical detectors and an oscilloscope are used to digitise the signals [6, 7]. The beam position is then calculated using

$$x = K_x \frac{\Delta}{L + R}, \quad (1)$$

where  $x$  is the beam position, and  $K_x$  is a geometric scaling factor [8].

\* daniel.harryman@cern.ch

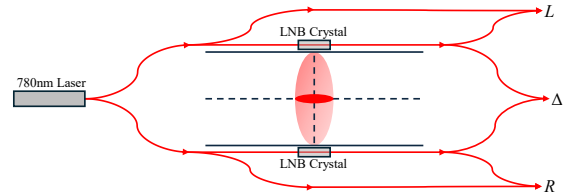


Figure 1: EO-BPM MZ interferometer configuration used in the SPS [1].

## LIMITATIONS

Electro-Optical (EO) systems are well-suited for accelerator environments due to their resistance to electrical noise and their rapid response time [9]. However, employing EO-BPM pickups in an interferometric configuration, as shown in Fig. 1, presents challenges related to dynamic range and baseline stability.

### Dynamic Range

The output of each MZ interferometer is given by

$$V = A + B \cos \left( \phi_0 + \pi \frac{E}{E_\pi} \right), \quad (2)$$

where  $A$  is the offset,  $B$  the fringe amplitude,  $\phi_0$  the initial phase,  $E_\pi$  the electric field strength in a crystal required for a phase shift of  $\pi$ , and  $E$  is given by:

$$E = \begin{cases} E_l, & \text{for the left side-mode interferometer} \\ E_r, & \text{for the right side-mode interferometer} \\ E_l - E_r, & \text{for the difference interferometer} \end{cases}$$

with  $E_l$  and  $E_r$  being the fields in the left and right crystals, respectively.

An initial phase of  $90^\circ$  gives a sine response with maximum pseudo-linear range. As  $E$  increases, the response becomes non-linear and can invert (over-rotate), leading to ambiguity due to the system's periodic nature and hence limiting the dynamic range.

### Stability

The initial phase of each EO-BPM interferometer in the SPS drifts independently at rates in the order of 1 rad/s [1], making it difficult to compare side-mode and difference channels without active stabilisation. While [1] describes a feedback system that stabilises one interferometer by tuning the laser wavelength, this method cannot be applied to all

three simultaneously, as correcting for one interferometer introduces instability in the others.

## INTERFEROMETER STABILISATION

Figure 2 shows a schematic of a single side-mode interferometer with an external phase modulator for stability control. The optical coupler provides two outputs: in-phase and anti-phase. The in-phase output is measured by a wideband photodetector (DC–12 GHz) and digitised with an oscilloscope [10]. The anti-phase output is measured by a slower photodetector and filtered with a 1 kHz low-pass filter to extract the DC level. This level is sent to a feedback controller, which adjusts the modulator bias to maintain a constant DC level, thereby stabilising the initial phase offset. Changing the DC set-point locks the system to a new initial phase.

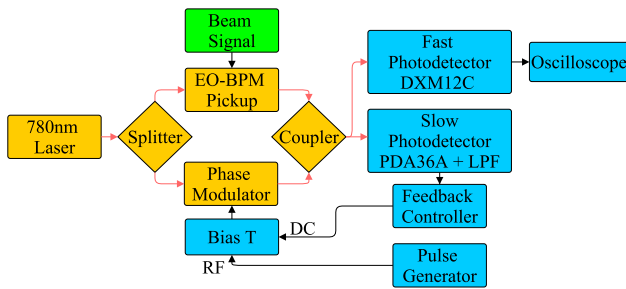


Figure 2: EO-BPM side-mode MZ interferometer configuration using an external phase modulator for active stabilisation control and system identification.

In addition to a stabilising bias voltage, an RF signal is injected to the same phase modulator via a bias-tee. The RF input of the bias-tee is connected to a pulse generator, allowing for signal injection for system identification and calibration. By applying a linear ramp input, a full rotation of the MZ response can be induced and measured. From this, the initial phase, fringe amplitude and signal offset from Eq. (2) are extracted.

## IQ DEMODULATION

### Theory

A method of improving the dynamic range is to use a 90° optical hybrid and In-Phase Quadrature (IQ) demodulation techniques [11]. This involves measuring the same beam modulated signal at two initial phases offset by 90°. Expanding Eq. (2) with two channels offset by 90° gives the outputs of

$$V_1 = A_1 + B_1 \cos\left(\phi - \frac{\pi}{2}\right) = A_1 + B_1 \sin(\phi), \quad (3)$$

$$V_2 = A_2 + B_2 \cos(\phi), \quad (4)$$

where

$$\phi = \pi \frac{E}{E_\pi}. \quad (5)$$

Using the RF input of a bias-tee shown in Fig. 2 a ramp voltage is input to force an over-rotation and measure the full

phase response of the channel. Performing this operation for both channels the  $A$  and  $B$  terms are obtained, the IQ components are then calculated using

$$I = \frac{V_1 - A_1}{B_1} = \sin(\phi), \quad (6)$$

$$Q = \frac{V_2 - A_2}{B_2} = \cos(\phi). \quad (7)$$

Finally the phase shift is recovered using

$$\phi = \arctan\left(\frac{I}{Q}\right). \quad (8)$$

For larger phase shifts, the phase is extracted using a phase unwrapping algorithm. In order for such an algorithm to reliably extract the correct phase, the following condition must be satisfied:

$$|\phi_{n+1} - \phi_n| < \pi, \quad (9)$$

where  $n$  denotes the sample number [12].

Figure 3 shows a single EO-BPM side-mode configuration capable of IQ detection using two MZ interferometers. This configuration splits the EO-BPM pickup output in Fig. 2 and combines it with the output from a second phase modulator. Collectively, the optical splitters and phase modulators form a 90° degree optical hybrid built from discrete components [11].

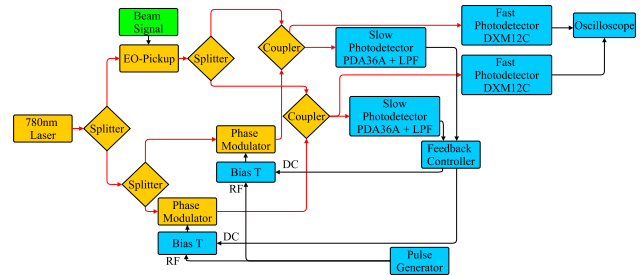


Figure 3: EO-BPM side-mode dual MZ interferometer configuration for IQ detection.

## EXPERIMENTAL SETUP AT CLEAR

The IQ read-out technique was tested using a single EO-BPM pickup and the configuration shown in Fig. 3, where the EO-BPM pickup and body were reused from a previous experiment [2]. The body was mounted on an optical breadboard along with the optical system. This breadboard was attached to a linear stage and installed in the in-air test stand at the CLEAR accelerator. The linear stage was used to simulate changes in beam position by varying the impact parameter, defined as the distance between the centre of the extracted beam and the pickup.

For these experiments, CLEAR extracted 220 MeV electron bunches with bunch length  $\sigma \approx 2$  ps and bunch charge in the range 0.1–0.17 nC. A function generator was set up to deliver ramped pulses to the RF input of each bias-tee using a trigger delayed to that of the oscilloscope. This enables the measurement of beam signals with a calibration ramp in the same acquisition trace.

## RESULTS

### Extraction Trace

Figure 4 shows a trace measured from a single bunch extraction taken at an impact parameter of 1 mm with the unwrapped phase data. The short peak seen in Fig. 4 at approximately 302 ns is the bunch signal. The sinusoidal responses in  $V_1$  and  $V_2$  seen from approximately 330 ns are the responses to the calibration ramp. The unwrapped phase is calculated by using Eqs. (6), (7) and (8) and performing an offset subtraction. This shows that the IQ demodulation technique can be used to successfully obtain the phase shift caused by the bunch and recover the calibration ramp signal from the two channels.

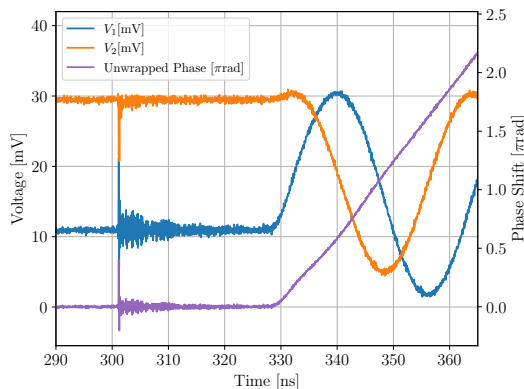


Figure 4: Single bunch trace measured at an impact parameter of 1 mm.

### Position Scan

A position scan was taken where the beam was set to a bunch charge of approximately 0.16 nC, the position was varied from an impact parameter of 1 to 30 mm by moving the linear stage. At each position, twenty bunches were recorded, with any that lost feedback stabilisation in either interferometer excluded from the analysis.

Using the bunch charge recorded for each bunch the acquired beam signals of  $V_1$  and  $V_2$  were linearly normalised to a bunch charge of 0.16 nC. The  $V_1$  and  $V_2$  signals were converted into  $I$  and  $Q$ , the difference between the bunch signal peak and the baseline was then extracted. To produce the phase shift the  $V_1$  and  $V_2$  signals without charge normalisation were converted into  $I$  and  $Q$ , these were processed into the unwrapped phase shift, the difference from the phase shift peak and the baseline was extracted and normalised to a bunch charge of 0.16 nC. The normalised  $I$ ,  $Q$  and unwrapped phase are all presented vs the impact parameter in Fig. 5.

Figure 5 shows that at large impact parameters, the  $I$  channel signal is low but detectable. At low impact parameters, where the gradient should peak, the  $I$  channel instead shows a reduced gradient. Conversely, the  $Q$  channel only responds for impact parameters below 20 mm, with its gradient increasing at the lowest values. These effects arise from the

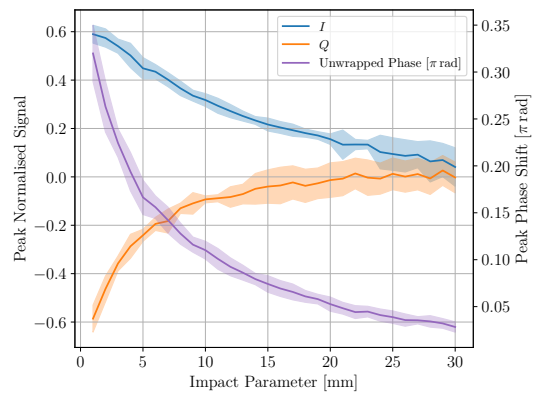


Figure 5: Position Response normalised to 0.16 nC. The error bars represent one standard deviation of the dataset used for each impact parameter.

sinusoidal response of the MZ interferometers convolved with the single pickup response [13].

Combining the  $I$  and  $Q$  values into an unwrapped phase shift leverages the strengths of both channels. Like the  $I$  channel, the phase shift signal remains visible at large impact parameters, while also exhibiting the increased gradient at low impact parameters characteristic of the  $Q$  channel. This results in a more accurate representation of the EO-BPM pickup response.

## CONCLUSION

This paper presents the successful demonstration of stabilising a single MZ interferometer, injecting calibration ramps for system identification, and implementing an interferometer configuration for IQ detection to increase dynamic range.

Extending IQ detection to a full EO-BPM system significantly complicates the setup. Instead of three interferometers required to measure beam position, six would be needed. Some of this complexity could be mitigated by moving the laser wavelength to 1550 nm, where off-the-shelf 90° optical hybrids are available as integrated components [14].

To fully capitalise on the benefits of an IQ detection system, the EO-BPM pickup should be purposefully designed with this architecture in mind. The phase shift induced in an LNB crystal is linearly proportional to its length [3]. Currently, this length is selected as a compromise: it is long enough to provide sufficient phase shift for injected beams, but short enough to avoid over-rotation for extracted beams. With IQ detection, longer modulators can be used, as over-rotated signals are accurately recovered. In turn this improves sensitivity in the low phase-shift regime.

## ACKNOWLEDGEMENTS

Acknowledgements and thanks are given to the CLEAR operations team. This work has been supported by UK STFC grants ST/N001583/1, ST/P00203X/1.

## REFERENCES

- [1] M. Z. C. Bosman *et al.*, “Design and Deployment of an In-Vacuum Electro-Optic BPM Pickup at the CERN SPS”, in *Proc. IBIC’24*, Beijing, China, Sep. 2024, pp. 161–165. doi:10.18429/JACoW-IBIC2024-TUP46
- [2] S. M. Gibson *et al.*, “Electro-Optical BPM Development for High Luminosity LHC”, in *Proc. IBIC’22*, Kraków, Poland, Sep. 2022, pp. 181–185. doi:10.18429/JACoW-IBIC2022-TU1I1
- [3] A. Arteché *et al.*, “Beam Measurements at the CERN SPS Using Interferometric Electro-Optic Pickups”, in *Proc. IBIC’19*, Malmö, Sweden, Sep. 2019, pp. 457–460. doi:10.18429/JACoW-IBIC2019-WEA004
- [4] A. Arteché *et al.*, “First Beam Tests at the CERN SPS of an Electro-Optic Beam Position Monitor for the HL-LHC”, in *Proc. IBIC’17*, Grand Rapids, MI, USA, Aug. 2017, pp. 270–273. doi:10.18429/JACoW-IBIC2017-TUPCF23
- [5] A. Arteché *et al.*, “Development of a Prototype Electro-Optic Beam Position Monitor at the CERN SPS”, in *Proc. IBIC’16*, Barcelona, Spain, Sep. 2016, pp. 634–637. doi:10.18429/JACoW-IBIC2016-WEPG09
- [6] Thorlabs, RXM10CFA – Single Mode Ultrafast Receiver, 700–870 nm, 40 kHz–10 GHz, FC/PC. <https://www.thorlabs.com/thorproduct.cfm?partnumber=RXM10CF>
- [7] Keysight Technologies, DSOS404A – Infiniium S-Series High-Definition Oscilloscope, 4 GHz, 4 Analog Channels. <https://www.keysight.com/zz/en/product/DSOS404A/high-definition-oscilloscope-4-ghz-4-analog-channels.html>
- [8] H. Schmickler, “Beam Position Measurement System Design”, in *Proc. IBIC’15*, Melbourne, Australia, Sep. 2015, pp. 618–624. doi:10.18429/JACoW-IBIC2015-THALA01
- [9] A. Schlögelhofer *et al.*, “Remote Sensing of Fast Beam Signals Using Electro-optical Modulators”, in *Proc. IBIC’24*, Beijing, China, Sep. 2024, pp. 219–223. doi:10.18429/JACoW-IBIC2024-WEA12
- [10] Thorlabs, DXM12CF – Single-Mode Ultrafast Detector with Current Monitor, 700–870 nm, DC–12 GHz, FC/PC. <https://www.thorlabs.com/thorproduct.cfm?partnumber=DXM12CF>
- [11] Z. Wang *et al.*, “Coherent  $\Phi$ -OTDR based on I/Q demodulation and homodyne detection,” *Opt. Express*, vol. 24, no. 2, pp. 853–858, Jan. 2016, doi:10.1364/OE.24.000853
- [12] A. Baldi, F. Bertolino, and F. Ginesu, “Phase Unwrapping Algorithms: A Comparison”, in *Interferometry in Speckle Light*, P. Jacquot and J.-M. Fournier, Eds. Berlin, Heidelberg: Springer, 2000, pp. 483–490. doi:10.1007/978-3-642-57323-1\_59
- [13] A. A. Nosych, U. Iriso, A. Olmos, and M. Wendt, “Overview of the Geometrical Non-Linear Effects of Button BPMs and Methodology for Their Efficient Suppression”, in *Proc. IBIC’14*, Monterey, CA, USA, Sep. 2014, paper TUPF03, pp. 298–302.
- [14] 90° Optical Hybrid for Space Applications – Datasheet, Exail. <https://www.exail.com/product/90-optical-fibers-coh-photonics-space>